Theoretical possibilities for the Peierls instability in polyalkylsilene

Kyozaburo Takeda
Basic Research Laboratories, Nippon Telegraph and Telephone Corporation, Musashino-shi, Tokyo 180, Japan

Seiichi Kagoshima
College of General Education, University of Tokyo, Komaba, Tokyo, Japan

(Received 4 June 1987)

Energy-band structures have been calculated for $+SiR+_x$ polyalkylsilene model compounds, where R indicates an H atom or a CH_3 [methyl (Me)] group. A possible Peierls instability has also been investigated theoretically for these polymers. Polyalkylsilene with H-atom or Me side groups have overlapped conduction bands formed of skeleton π bands and σ bands. This band overlapping suppresses the metal-insulator (M-I) transition due to the simple double-bond alternation found in $+CH+_x$. This band overlapping also causes three types of scattering processes: Two of them are intra-σ-band and intra-π-band scatterings and the other is inter-σ-π-band scattering. Inter-σ-π-band scattering produces a charge-density wave (CDW) having a commensurate wave number of $q_{\sigma\pi}=\pi/a$ by dimerizing two skeleton unit cells. Intra-σ-band scattering produces a CDW having an incommensurate wave number of $q_\sigma=2k_F^\sigma$. However, this incommensurate CDW is equivalent to an incommensurate CDW with $q_\pi=2k_F^\pi$ produced by intra-π-band scattering, because the one dimensionality of overlapping band guarantees the relation of $k_F^\sigma+k_F^\pi=\pi/a$. The resulting polyalkylsilene tends to have the characteristics of an insulator due to intraband scattering rather than interband scattering. This is because of its orthogonality of overlapping σ and π bands.

I. INTRODUCTION

Polysilene[1] is a hypothetical polyene whose structure is analogous to polyacetylene. While the latter has C double bonds along the skeleton, the former has Si double bonds along the skeleton. The formation of π bonding between Si atoms has been recently investigated. Pandey[2] proposed the π-bonded Si chain so as to interpret the the Si-surface characteristics. Chemically, small but stable oligomers having Si=Si double bonds have been synthesized.[3] A theoretical calculation[4] also shows that polysilene catena has a possibility of forming overlapping conduction bands. Thus polysilene is a hypothetical polyene yet, this is, however, an important model polyene not only for the systematic investigation of group-IV polyene but also for the model investigation of Peierls instability in the novel polyene with overlapping multiband structure.

This paper concerns a theoretical investigation of some possible ideas for such Peierls instabilities in the overlapping multiband, via the case of polyalkylsilene. For this purpose we first focus on the electronic structure of polyalkylsilene, $+SiR+_n$, where R indicates an H atom or Me (methyl) group (Fig. 1). It is assumed to have a transplanar zigzag chain from drawing an analogy with polyacetylene. Section II includes the results of theoretical calculations of the electronic structure for $(SiR)_n$. This section also discusses the influence of bond alternation upon the electronic structure. The resulting band overlapping found in polyalkylsilene has a possibility to suppress a metal-insulator (M-I) transition due to such a simple double-bond alternation.[4] Therefore, possible Peierls instabilities in the overlapped multiband structure should be investigated. We then discuss the electron-phonon interaction occurring in this characteristic band structure and also estimate the corresponding coupling constants in terms of the deformation-potential approximation in Sec. III. Section IV deals with a theoretical in-

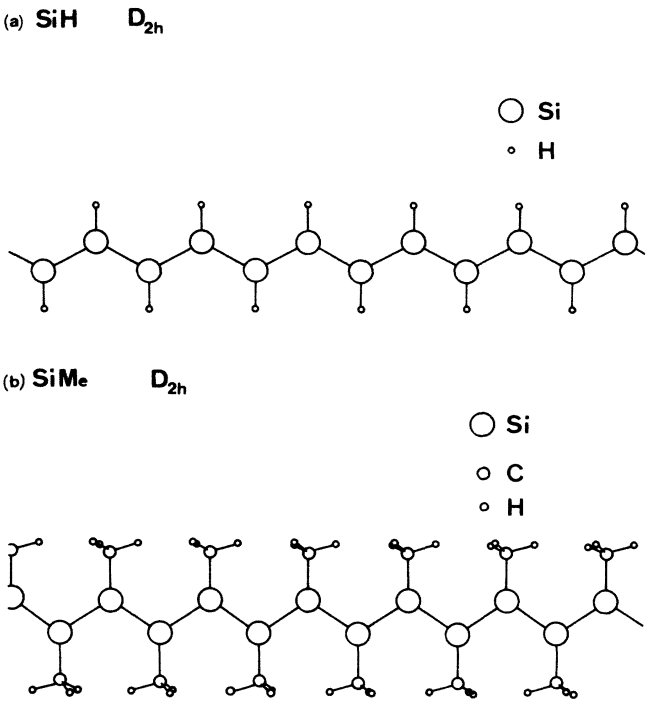

FIG. 1. Illustration of (a) $(SiH)_x$ and (b) $(SiMe)_x$.

vestigation of the *M-I* Peierls transitions as well as the phonon softening due to the Kohn anomaly in these polyalkylsilenes. We also discuss the qualitative influence of the side-group methylation upon both the band structure and the *M-I* Peierls transition mechanism by comparing the results of $(SiH)_x$ and $(SiMe)_x$.

II. ELECTRONIC STRUCTURE OF POLYALKYLSILENE

A. Energy-band structure of polyalkylsilene

A semiempirical band calculation method known to describe the band-edge structure was used.[5] The method is based on the linear-combination-of-atomic-orbitals method (LCAO) approach of Slater and Koster (SK),[6] because of the covalency in polysilene. The valence-orbital approximation is known to provide a good approximation for Si and C elements. Therefore, the valence eigenfunctions of Si $3s$, Si $3p_x$, Si $3p_y$, Si $3p_z$, C $2s$, C $2p_x$, C $2p_y$, C $2p_z$, and H $1s$ atomic orbitals (AO's) can be employed as the basis in this calculation. The wave function for an electron in a polymer can be expressed in terms of Bloch sums of the eigenfunctions ϕ_l^α of the bound state of free atoms:

$$\Psi_{\mathbf{k}}^j(\mathbf{r})=\sum_{\mathbf{R}_n} e^{i\mathbf{k}\cdot\mathbf{R}_n}\sum_{l,\alpha} C_{l\alpha}^{j\mathbf{k}}\phi_l^\alpha(\mathbf{r}-\mathbf{R}_n)\ . \tag{2.1}$$

Here, $\mathbf{R}_n$ means a positional vector for the nth lattice. The sum over eigenfunctions should be over both atomic species α involved in the unit cell and over the quantum state (l) of the corresponding AO. $C_{l\alpha}^{j\mathbf{k}}$ indicates an expansion coefficient for the jth eigenstate. According to the conventional variation technique, the following familiar secular equation can be obtained:

$$\left|\varepsilon_i\sum_{\mathbf{R}_n} e^{i\mathbf{k}\cdot\mathbf{R}_n}\langle\phi_{j(\mathbf{r}-\mathbf{R}_n)}\mid\phi_{i(\mathbf{r})}\rangle+\sum_{\mathbf{R}_n} e^{i\mathbf{k}\cdot\mathbf{R}_n}\langle\phi_{j(\mathbf{r}-\mathbf{R}_n)}\mid\hat{H}\mid\phi_{i(\mathbf{r})}\rangle-E\sum_{\mathbf{R}_n} e^{i\mathbf{k}\cdot\mathbf{R}_n}\langle\phi_{j(\mathbf{r}-\mathbf{R}_n)}\mid\phi_{i(\mathbf{r})}\rangle\right|=0\ . \tag{2.2}$$

The symbol $\langle\phi_j\mid\hat{H}\mid\phi_i\rangle$ is an interatomic matrix element (or LCAO parameter), which is estimated here by Harrison's method.[7] In his formation, the interatomic matrix elements can be expressed as

$$\langle\phi_j\mid\hat{H}\mid\phi_i\rangle=E_{ij\kappa(uvw)}=\eta_{ll'm}\frac{\hbar^2}{m_0 d^2}\ , \tag{2.3}$$

where κ represents σ or π bonding and d is the interatomic matrix distance. The subscripts u, v, and w are direct cosines for positional vector $\mathbf{R}_n$. The symbols l and l' on the right-hand side indicate the azimuthal quantum number for individual atomic orbitals labeled by $s(l=0)$ or $p(l=1)$, and m is the magnetic quantum number labeled by $\sigma(m=0)$ or $\pi(m=1)$. The parameter $\eta_{ll'm}$ is the Harrison coefficient.

The symbol ε_i in Eq. (2.2) represents the on-site energy. In chainlike polymers, these values are different from those for an isolated atomic Hamiltonian [e.g., the result of Herman and Skillman (HS)] due to the formation of the chain structure. Therefore, the adjusted HS ε_i values[5] for Si, C, and H are used for the calculation. These values produce reasonable ionization-potential (IP) values.

Figure 2 shows the calculated energy-band structures near the Fermi level of $(SiH)_x$. Double bonds are assumed to be fully delocalized along the skeleton to form D_{2h} symmetry. Characteristic of the conduction band (CB) is an overlapping between the π and σ bands. The resulting Fermi level intersects these two overlapping CB's. A metallic state is then produced.[4] This feature is caused by inherently small band gaps of Si-skeleton polymers, less than half of those of C-skeleton polymers. The overlapping CB states are composed of skeleton Si AO's and are delocalized along the Si skeleton; the bottom state of the π band is a bonding π state between Si $3p_z$ AO's whose lobes stand vertically on the skeleton plane, and the bottom state of the σ band is an antibonding σ state between Si $3s$ AO's. The Si $3p_y$ AO's are also admixtured in the σ-band state.

Figure 3 shows the calculated energy-band structures of $(SiH)_x$ when a strong bond alternation occurs.[4] Simple bond alternation does not result in variation in the unit cell but lowers the symmetry of the chain from D_{2h} to C_{2h}. This reduction in symmetry removes the energy de-

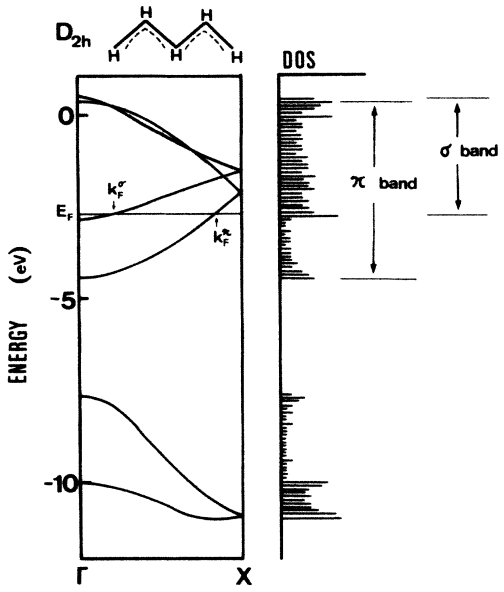

FIG. 2. Calculated energy-band structure of $(SiH)_x$ with delocalized skeleton double bonds. Length of double bond is average of experimental values of Si—Si (2.346 Å) and Si=Si (2.16 Å) double bonds.

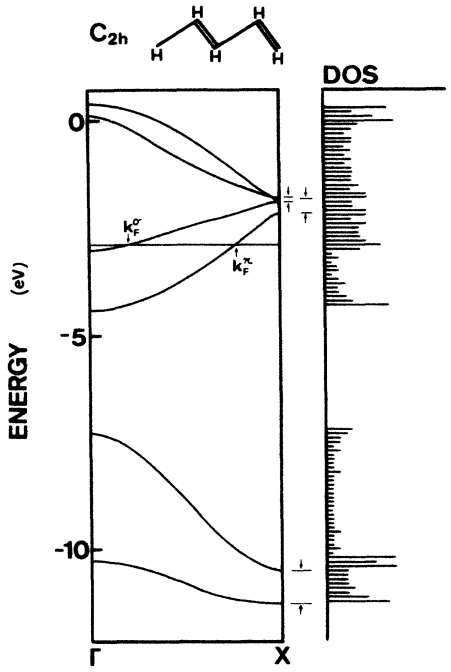

FIG. 3. Calculated energy-band structure of $(SiH)_x$ having bond-alternation skeleton.

generacies at point X. However, the inherently long length of interatomic distances between Si atoms reduces the difference between single bond (Si—Si) and double bond (Si=Si) lengths. This inconspicuous difference results in band splittings at point X small enough that the resulting Fermi surface still intersects both the π and σ bands. This result, that the commensurate-lattice displacement due to the bond alternation produces no M-I transition, is quite different from the $+CH+_x$ system.

A quite similar band structure near the Fermi level is also obtained when the side groups are substituted from H to Me (methylation), because the corresponding electronic states are mainly determined by Si-skeleton AO's. Therefore, polyalkylsilenes would tend to maintain a metallic character even after simple bond alternation.

B. Overlapping multiband model for polyalkylsilene

The resulting conduction bands of polyalkylsilene have an overlapping multiband structure between the π and σ bands near the Fermi surface. For simplicity of the following considerations, we describe these two bands in terms of a parabolic band with the effective-mass approximation (m_σ and m_π) in Fig. 4.

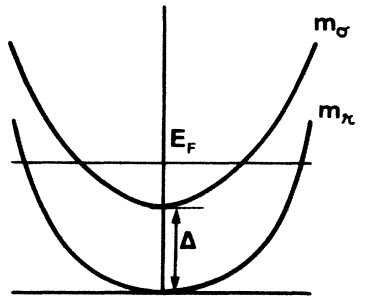

FIG. 4. Illustration of an overlapping two-band model.

The E^i-k dispersion and the density of states (DOS) g^i for the π band ($i=\pi$) are expressed as

$$E^{\pi}_{(k)}=\frac{\hbar^2}{2m_\pi}k^2\,,$$
$$g^{\pi}_{(E)}=\frac{2}{2\pi}\left[\frac{2m_\pi}{\hbar^2}\right]^{1/2}\frac{1}{\sqrt{E}}\,. \tag{2.4}$$

Those for the σ band ($i=\sigma$) are

$$E^{\sigma}_{(k)}=\frac{\hbar^2}{2m_\sigma}k^2+\Delta\,,$$
$$g^{\sigma}_{(E)}=\frac{2}{2\pi}\left[\frac{2m_\sigma}{\hbar^2}\right]^{1/2}\frac{1}{\sqrt{E-\Delta}}\,, \tag{2.5}$$

where Δ is an energy difference between two bands. The total DOS g^t is then

$$g^{t}_{(E)}=\begin{cases} g^{\pi}_{(E)}\,, & 0\le E\le\Delta \\ g^{\pi}_{(E)}+g^{\sigma}_{(E)}\,, & E>\Delta\,. \end{cases} \tag{2.6}$$

The overlapping of the half-filled π band over the empty σ band causes electrons to flow from the π band toward the σ band. This flow of electrons lowers the Fermi energy E_F. The lowered E_F is approximately determined[8] by the above band parameters (effective-mass ratios of m^*_σ and m^*_π, and energy difference Δ) and the electron number density n ($=2k_{F_0}/\pi$):

$$E_F=\begin{cases} \dfrac{\hbar^2}{2m_0}\dfrac{[(m^*_\pi+m^*_\sigma)k^2_{F_0}-(m^*_\pi-m^*_\sigma)m^*_\sigma(2m_0/\hbar^2)\Delta]-2k_{F_0}\{m^*_\pi m^*_\sigma[k^2_{F_0}-(m^*_\pi-m^*_\sigma)(2m_0/\hbar^2)\Delta]\}^{1/2}}{(m^*_\pi-m^*_\sigma)^2} & (m^*_\sigma\neq m^*_\pi)\,, \\ \dfrac{\hbar^2}{2m_0}\dfrac{k^2_{F_0}+m^*(2m_0/\hbar^2)\Delta}{4m^*k^2_{F_0}} & (m^*_\sigma=m^*_\pi\equiv m^*)\,, \end{cases} \tag{2.7}$$

and the corresponding Fermi wave numbers for the π and σ bands are

$$k_F^{\pi}=\pm\left[\frac{2m_{\pi}}{\hbar^2}\right]^{1/2}(E_F)^{1/2}\ ,$$
$$k_F^{\sigma}=\pm\left[\frac{2m_{\sigma}}{\hbar^2}\right]^{1/2}(E_F-\Delta)^{1/2}\ . \tag{2.8}$$

The values of the effective masses[9] for the σ and π bands were calculated for the resulting E^i-k dispersion of the band calculations (Sec. II A) in terms of the polynomial least-squares method. The resulting band parameters are tabulated in Table I.

III. ELECTRON-PHONON INTERACTION IN POLYALKYLSILENE

A. Equation of motion for overlapping multiband

The electrons and phonons are coupled via $H_{e\text{-ph}}$; as a result the phonon field acts to induce a certain density fluctuation in the electron system. This induced density fluctuation in turn affects the phonon field, since it serves to alter phonon frequencies. The calculation of the induced density fluctuations and the phonon dispersion relation should therefore be carried out in a self-consistent fashion.[10]

The normal-mode phonon oscillator amplitude Q_q without electron-phonon interaction is determined by the following equation of motion:

$$\ddot{Q}_q=-w_q^2Q_q\ . \tag{3.1}$$

When electrons with state $|k\rangle$ of the ith band interact with the phonons via the wave number q, and are then scattered to the state $|k'\rangle=|k+q\rangle$ of the jth band, the corresponding electron-phonon interaction $\hat{H}^{ij}_{e\text{-ph}}$ is expressed as

$$\hat{H}^{ij}_{e\text{-ph}}=\frac{1}{\sqrt{N}}\sum_q v_q^{ij}C_{q+k}^{j\dagger}C_k^i(b_q+b^{\dagger}_{-q})=\sum_q g_q^{ij}\rho_q^{ij}Q_q\ . \tag{3.2}$$

The symbols C^i and $C^{j\dagger}$ indicate an annihilation and creation operator for electrons in the ith and jth bands, respectively. The symbols b and $b^{\dagger}$ also indicate a corresponding operator for phonons. The total electron-phonon interaction $H_{e\text{-ph}}$ for the overlapping multiband system is obtained as

$$\hat{H}_{e\text{-ph}}=\sum_{i,j}\hat{H}^{ij}_{e\text{-ph}}=\sum_{i,j}\sum_q g_q^{ij}\rho_q^{ij}Q_q\ , \tag{3.3}$$

TABLE I. Band parameters of $(SiH)_x$ and $(SiMe)_x$ for the overlapping band model.

	m_{σ}^*	m_{π}^*	Δ (eV)
SiH	0.785	0.926	1.642
SiMe	0.603	0.986	1.239

where ρ_q^{ij} is the electron density operator and g_q^{ij} is the electron-phonon coupling term.

Since a typical phonon frequency is very small compared to a typical electron frequency, the coupling of electrons to phonons may be treated as a polarization process, in which phonons are regarded as an external field only weakly coupled to the electron gas. Then, this electron-phonon interaction plays the role of an outfield force $F_{e\text{-ph}}$ for Q_q,

$$F_{e\text{-ph}}=-\frac{\partial}{\partial Q_q}H_{e\text{-ph}}=-\sum_{i,j}g_q^{ij}\rho_q^{ij}\ . \tag{3.4}$$

Considering the electron-phonon interaction, the resulting equation of motion is then

$$\ddot{Q}_q=-w_q^2Q_q-\sum_{i,j}g_q^{ij}\rho_q^{ij}\ . \tag{3.5}$$

Let us now take the expectation value of both sides of this operator equation with respect to the electron coordinates:

$$\langle\ddot{Q}_q\rangle=-w_q^2\langle Q_q\rangle-\sum_{i,j}g_q^{ij}\langle\rho_q^{ij}\rangle\ . \tag{3.6}$$

The corresponding value for electron density $\langle\rho_q^{ij}\rangle$ is zero in the absence of a phonon field. In the presence of a field, the electron response may be specified with the aid of the response function $\chi^{ij}_{(q,T)}$ to the extent that the electrons respond linearly. The expectation value of ρ_q^{ij} is then

$$\langle\rho_q^{ij}\rangle=-\chi^{ij}_{(q,T)}\varphi_q^{ij}\ . \tag{3.7}$$

Here, φ^{ij} is the Fourier transform in space and time of scalar potential $\varphi^{ij}_{(r)}$, which acts on the system density of i- and j-band electrons through the interatomic Hamiltonian, $\hat{H}^{ij}_{e\text{-ph}}$,

$$\hat{H}^{ij}_{e\text{-ph}}=\sum_q\int\frac{d\omega}{2\pi}(\rho_q^{ij})^{\dagger}\varphi_q^{ij}e^{-i\omega t}\ . \tag{3.8}$$

From Eqs. (3.3) and (3.8), φ_q^{ij} is given as

$$\varphi_q^{ij}=\overset{*}{g}{}^{ij}_q\langle Q_q\rangle\ . \tag{3.9}$$

The resulting density fluctuation induced by a longitudinal field of average amplitude $\langle Q_q\rangle$ is simply

$$\langle\rho_q^{ij}\rangle=-\overset{*}{g}{}^{ij}_q\chi^{ij}_{(q,T)}\langle Q_q\rangle\ . \tag{3.10}$$

The equation of motion is then rewritten as

$$\langle\ddot{Q}_q\rangle=-\left[w_q^2-\sum_{i,j}|g_q^{ij}|^2\chi^{ij}_{(q,T)}\right]\langle Q_q\rangle\equiv\Omega_q^2\langle Q_q\rangle\ . \tag{3.11}$$

The phonon frequency Ω_q is reduced by the electron-phonon interaction by

$$\sum_{i,j}|g_q^{ij}|^2\chi^{ij}_{(q,T)}\langle Q_q\rangle\ . \tag{3.12}$$

B. Intraband and interband response functions

The response function for the multiband structure, $\chi^{ij}_{(q,T)}$, is defined by

$$\chi^{ij}_{(q,T)}=\frac{1}{N}\sum_k \frac{f^i_k-f^j_{k+q}}{E^j_{k+q}-E^i_k}=\frac{1}{\pi n}\int \frac{f^i_k-f^j_{k+q}}{E^j_{k+q}-E^i_k}dk \ . \tag{3.13}$$

First, we calculate this response function of the overlapping band model for the special case with $\Delta=0$ (Sec. II B) and $T=0$ K in order to investigate characteristics for intraband and interband scattering.

The intraband response function $\chi^{ij}_{(q,T)}$ is rewritten for the parabolic band with the effective mass m_i as

$$\chi^{ii}_{(q,T)}=\frac{1}{\pi n}\frac{2m_i}{\hbar^2}\frac{1}{q}\int \frac{f^i_k-f^i_{k+q}}{2k+q}dk \ . \tag{3.14}$$

The corresponding response function for an interband scattering $\chi^{ij}_{(q,T)}$ is

$$\chi^{ij}_{(q,T)}=\frac{1}{\pi n}\frac{(m_i m_j)^{1/2}}{\hbar^2}\frac{1}{q} \times\int (f^i_k-f^j_{k+q})\left[\frac{1}{k+aq}-\frac{1}{k+bq}\right]dk \ , \tag{3.15}$$

with

$$a=\frac{(m_i)^{1/2}}{(m_i)^{1/2}-(m_j)^{1/2}} \ ,$$

and

$$b=\frac{(m_i)^{1/2}}{(m_i)^{1/2}+(m_j)^{1/2}} \ .$$

Only for the limiting case of $T=0$ K can the response functions for both intraband and interband scattering be analytically calculated. The resulting intraband response function $\chi^{ii}_{(q,T=0)}$ is well known as

$$\chi^{ii}_{(q,T=0)}=\frac{1}{\pi n}\frac{2m_i}{\hbar^2}\frac{1}{q}\ln\left|\frac{q+2k^i_F}{q-2k^i_F}\right| \quad (i=\sigma \text{ or } \pi) \ . \tag{3.16}$$

When electrons are scattered from one Fermi point ($\pm k^i_F$) to another point ($\mp k^i_F$) within the same ith band, $\chi^{ii}_{(q,T=0)}$ has a logarithmically divergent value.

The interband response function $\chi^{ij}_{(q,T=0)}$ can also be expressed analytically when $T=0$ K:

$$\chi^{ij}_{(q,T=0)}=-\frac{1}{\pi n}\frac{(m_i m_j)^{1/2}}{\hbar^2}\frac{1}{q}\ln\left|\frac{k^i_F+aq}{k^i_F-aq}\frac{k^i_F-bq}{k^i_F+bq}\frac{k^j_F-(a-1)q}{k^j_F+(a-1)q}\frac{k^j_F-(1-b)q}{k^j_F+(1+b)q}\right| \ . \tag{3.17}$$

Since k^i_F and k^j_F are the Fermi wave numbers of the i and j bands, respectively, the following relation is obtained:

$$E_F=\frac{\hbar^2}{2m_i}(k^i_F)^2=\frac{\hbar^2}{2m_j}(k^j_F)^2 \ . \tag{3.18}$$

Therefore, Eq. (3.17) is rewritten as

$$\chi^{ij}_{(q,T=0)}=\frac{1}{\pi n}\frac{2(m_i m_j)^{1/2}}{\hbar^2}\frac{1}{q}\ln\left|\frac{q+(k^i_F+k^j_F)}{q-(k^i_F+k^j_F)}\right| \ . \tag{3.19}$$

Two possible phonon modes with $q^+_{ij}=k^\sigma_F+k^\pi_F$ and $q^-_{ij}=k^\sigma_F\sim k^\pi_F$ are apparently struck upon interband scattering in this overlapping multiband system. However, the latter process involving the q^- phonon mode is forbidden because the final electron state scattered by these phonons is already occupied. This is the reason that the interband scattering response function χ^{ij} [Eq. (3.19)] only has one singularity of the logarithmic divergence at $q^+_{ij}=k^\sigma_F+k^\pi_F=\pi/a$. Thus, a two-band overlapping system has three types of scattering processes; two of them are caused by intraband scattering ($\chi^{\pi\pi}$ and $\pi^{\sigma\sigma}$), and the other is due to interband scattering ($\chi^{\sigma\pi}$ or $\chi^{\pi\sigma}$).

As an analytical expression for $\chi^{ij}_{(q,T)}$ can only be obtained for $T=0$ K, we will hereafter numerically calculate the intraband and interband scattering response functions [Eq. (3.13)] using the overlapping two-band model (Sec. II B). In these numerical calculations, the infinite integral over k can be reduced to the finite integral near the Fermi surface because of the character of the Fermi-Dirac distribution function,

$$\chi_{(q,T)}=\int_{-\infty}^{\infty}\frac{f_k-f_{k+q}}{E_{k+q}-E_k}dk \sim\int_{-k_F-q-\xi_T}^{k_F+\xi_T}\frac{f_k-f_{k+q}}{E_{k+q}-E_k}dk \ . \tag{3.20}$$

Thermal fluctuation in the distribution is introduced in terms of $\xi_T\sim(k_BT)^{1/2}$. Moreover, we decomposed the above finite integral into several parts [Eq. (3.21)], paying attention to the divergent character of the integrated function at $q=-k_F$,

$$\int_{-k_F-q-\xi_T}^{k_F+\xi_T}dk=\int_{-k_F-q-\xi_T}^{-k_F-\xi_T}dk+\int_{-k_F-\xi_T}^{-k_F+\xi_T}dk+\int_{-k_F+\xi_T}^{k_F+\xi_T}dk \ . \tag{3.21}$$

Numerical calculations have been carried out using the adaptive Newton-Cotes nine-point rule.

C. Electron-phonon coupling for the overlapping multiband system

Electron-phonon coupling constants g^{ij}_q $(i,j=\sigma,\pi)$ should be determined in order to calculate the phonon frequency Ω_q of Eq. (3.11) numerically. We estimated these values by using the deformation-potential approximation.

In the deformation-potential representation, the electron-phonon interaction $\hat{H}_{e\text{-ph}}$ is

$$\hat{H}_{e\text{-ph}}=\sum_{i,j}\sum_{q}\left[\frac{\hbar}{2MN_I}\right]^{1/2}\Xi_{\text{eff}}^{ij}(q)\frac{i(\mathbf{e}_q\cdot\mathbf{q})}{(w_q)^{1/2}}(b_q+b_{-q}^{\dagger})\times\int n_{(\mathbf{r}')}^{ij}e^{i\mathbf{q}\cdot\mathbf{r}'}d\mathbf{r}'$$

$$=\sum_{i,j}\sum_{q}\Xi_{\text{eff}}^{ij}(q)\left[\frac{1}{MN_I}\right]^{1/2}i(\mathbf{e}_q\cdot\mathbf{q})Q_q\rho_q^{ij}\ . \tag{3.22}$$

Here,

$$\rho_q^{ij}=\int n_{(\mathbf{r}')}^{ii}e^{i\mathbf{q}\cdot\mathbf{r}'}d\mathbf{r}'=C_{q+k}^{j\dagger}C_k^i=\tilde{\rho}_q^{ij}I_{k\mu,k'\nu}^{ij}\quad(k'=k+q) \tag{3.23}$$

and $\tilde{\rho}_q^{ij}$ is the qth Fourier component of the electron density between the ith and jth bands having spherical orbital symmetry. The difference between intraband and interband scattering due to $C_{q+k}^{j\dagger}C_k^i$ can be represented in terms of an overlap integral $I_{k\mu,k'\nu}^{ij}$. This integral means the overlap between initial state $|k\rangle$ and final state $|k'\rangle$ and depends on the orbital symmetry. Therefore, the coupling constant g^{ij} including spin states is expressed in terms of the deformation potential $\Xi_{\text{eff}}^{ij}(q)$,

$$g_q^{ij}=\Xi_{\text{eff}}^{ij}(q)\left[\frac{1}{MN_I}\right]^{1/2}i(\mathbf{e}_q\cdot\mathbf{q})I_{k\mu,k'\nu}^{ij}\equiv\tilde{g}_q^{ij}I_{k\mu,k'\nu}^{ij}\ . \tag{3.24}$$

The reduction term of the phonon frequency Ω_q due to the electron-phonon coupling is rewritten as

$$\sum_{i,j}|g_q^{ij}|^2\chi_{(q,T)}^{ij}\langle Q_q\rangle=\sum_{i,j}\sum_{\mu,\nu}|g_q^{i\mu,j\nu}|^2\chi_{(q,T)}^{ij}\langle Q_q\rangle\ . \tag{3.25}$$

The sum over spin states (μ and ν) is rewritten as

$$\sum_{\mu,\nu}|g_q^{i\mu,j\nu}|^2=\tfrac{1}{2}(|g_q^{i\uparrow j\uparrow'}|^2+|g_q^{i\uparrow j\downarrow'}|^2+|g_q^{i\downarrow j\uparrow'}|^2+|g_q^{i\downarrow j\downarrow'}|^2)=|\tilde{g}_q^{ij}|^2G_{kk'}^{ij}\ , \tag{3.26}$$

with

$$G_{kk'\,(=k+q)}^{ij}=\tfrac{1}{2}(|I_{kk'}^{i\uparrow j\uparrow'}|^2+|I_{kk'}^{i\uparrow j\downarrow'}|^2+|I_{kk'}^{i\downarrow j\uparrow'}|^2+|I_{kk'}^{i\downarrow j\downarrow'}|^2)\ . \tag{3.27}$$

Therefore, the resulting reduction term is

$$\sum_{i,j}|g_q^{ij}|^2\chi_{(q,T)}^{ij}\langle Q_q\rangle=\sum_{i,j}|\tilde{g}_q^{ij}|^2G_{kk'}^{ij}\chi_{(q,T)}^{ij}\langle Q_q\rangle\ . \tag{3.28}$$

For a qualitative discussion, we estimate values of overlap functions G^{ij} for the special case of

$$\Delta=\frac{\hbar^2}{2m_\pi}(k_F^\pi)^2\ . \tag{3.29}$$

That is, the σ band just connects to the π band. At $T=0$ K, phonons cause transitions between the following four electronic states, $|\sigma_k\rangle$, $|\sigma_{k'}\rangle$, $|\pi_k\rangle$, and $|\pi_{k'}\rangle$.

Let directions k and k' be in the X and X' directions of the coordinate systems (X,Y,Z) and (X',Y',Z'), respectively. When ϕ and θ are the azimuthal and polar angles of k' with respect to coordinate system (X,Y,Z), spatial and spin coordinates have the following relations:

$$\begin{bmatrix}X'\\Y'\\Z'\end{bmatrix}=\begin{bmatrix}\cos\theta & \sin\theta\cos\phi & \sin\theta\sin\phi\\ -\sin\theta & \cos\theta\cos\phi & \cos\theta\sin\phi\\ 0 & -\sin\phi & \cos\theta\end{bmatrix}\begin{bmatrix}X\\Y\\Z\end{bmatrix},\qquad \begin{bmatrix}\uparrow'\\\downarrow'\end{bmatrix}=\begin{bmatrix}e^{-i\phi/2}\cos(\theta/2) & e^{i\phi/2}\sin(\theta/2)\\ -e^{-i\phi/2}\sin(\theta/2) & e^{i\phi/2}\cos(\theta/2)\end{bmatrix}\begin{bmatrix}\uparrow\\\downarrow\end{bmatrix}. \tag{3.30}$$

Since the one dimensionality of the considered system introduces $\theta=\pi$ and $\phi=0$, the resulting relations are rewritten as

$$\begin{bmatrix}X'\\Y'\\Z'\end{bmatrix}=\begin{bmatrix}-X\\-Y\\Z\end{bmatrix}\quad\text{and}\quad\begin{bmatrix}\uparrow'\\\downarrow'\end{bmatrix}=\begin{bmatrix}\downarrow\\-\uparrow\end{bmatrix}. \tag{3.31}$$

Therefore, the initial ($|\pi_k\rangle$ and $|\sigma_k\rangle$) and final ($|\pi_{k'}\rangle$ and $|\sigma_{k'}\rangle$) states are given for polyalkylsilene as

$$\begin{aligned}&|\pi_k,\mu\rangle\sim|\pi_X,\mu\rangle=|\pi_X\rangle\mu\quad(X=\pi/a)\ ,\\ &\qquad|\pi_X\rangle=C_{\pi_1}|3P_{z_1}\rangle+C_{\pi_2}|3P_{z_2}\rangle\ ,\\ &|\sigma_k,\mu\rangle\sim|\sigma_\Gamma,\mu\rangle=|\sigma_\Gamma\rangle\mu\ ,\\ &\qquad|\sigma_\Gamma\rangle\sim C_{\sigma_1}|3S_1\rangle+C_{\sigma_2}|3S_2\rangle\ ,\\ &|\pi_{k'},\mu\rangle\sim|\pi_{-X},\mu\rangle=|\pi_X\rangle\mu\ ,\\ &|\sigma_{k'},\mu\rangle\sim|\sigma_\Gamma,\mu\rangle=|\sigma_\Gamma\rangle\mu\qquad(|\pi_{-X}\rangle=|\pi_X\rangle)\ .\end{aligned} \tag{3.32}$$

The normality and orthogonality of the basis causes

$$\langle\sigma_\Gamma|\sigma_\Gamma\rangle=\langle\pi_X|\pi_X\rangle=1\quad\text{and}\quad\langle\sigma_\Gamma|\pi_X\rangle=\langle\pi_X|\sigma_\Gamma\rangle=0\ . \tag{3.33}$$

The resulting intraband and interband overlapping function G^{ij} are given as

$$G_{kk'}^{ii}=G_{kk'}^{\sigma\sigma}=G_{kk'}^{\pi\pi}=1$$

for intraband scattering, and

$$G_{kk'}^{ij}=G_{kk'}^{\sigma\pi}=G_{kk'}^{\pi\sigma}=0 \tag{3.34}$$

for interband scattering.

When the σ band goes down toward the π band (reduction in Δ), the positions of the Fermi wave numbers (k_F^σ and k_F^π) vary from those at the symmetric points (Γ and X) to the appropriate positions on the Δ axis in the Brillouin zone (Sec. II B). Nonorthogonal components between two bands are hybridized in $|\sigma_k\rangle$ and $|\pi_k\rangle$

states. However, the intraband overlap function $G^{ii}_{kk'}$ conserves the value of unity and the interband overlap function $G^{ij}_{kk'}$ also conserves the value of zero as long as the chain symmetrically hybridizes nonorthogonal components. This means that the orthogonality of overlapping bands tends to favor the intraband scattering rather than the interband scattering.

D. Deformation potentials in polyalkylsilene

Let us estimate the deformation potential of polyalkylsilene. In polyalkylsilene, it would be possible to treat lattice displacements due to phonons as changes in bond angles rather than changes in bond lengths because of its covalency. Since conduction electrons in both σ and π bands are delocalized along the skeleton axis, only such lattice displacements toward the skeleton axis are allowed to couple with those electrons in the overlapping CB states of polyalkylsilene. The reason is that the phonons interacting with electrons must be in their longitudinal modes within the N process. These displacements can be also simulated by varying the skeleton bond angles.

Changes in electron-energy eigenvalues are strongly dependent on the degree of orbital overlapping. Interatomic overlappings due to Si $3p_y$ AO components in the σ band are significantly affected by this skeleton deformation. On the contrary, corresponding interatomic overlappings in the π band are hardly influenced, because $3p_z$ AO's in the π band have a spherical symmetry in this variation in the skeleton bond angle. This results in larger changes in the former energy eigenvalues. The resulting intra-σ-band deformation potentials, $\Xi^{\sigma\sigma}_{\rm eff}$, are expected to be greater than $\Xi^{\pi\pi}_{\rm eff}$.

The deformation potentials $\Xi^{ij}_{\rm eff}$ are defined as

$$\Xi^{\pi\pi}_{\rm eff}(k^{\pi}_F)=\frac{|\Delta E^{\pi}(k^{\pi}_F)|}{\Delta_l} \tag{3.35}$$

for intra-π-band scattering,

$$\Xi^{\sigma\sigma}_{\rm eff}(k^{\sigma}_F)=\frac{|\Delta E^{\sigma}(k^{\sigma}_F)|}{\Delta_l} \tag{3.36}$$

for intra-σ-band scattering, and

$$\Xi^{\sigma\pi}_{\rm eff}(k^{\sigma}_F,k^{\pi}_F)=\frac{|\Delta E^{\sigma}(k^{\sigma}_F)-\Delta E^{\pi}(k^{\pi}_F)|}{\Delta_l} \tag{3.37}$$

for inter-σ-π-band scattering. Since electrons coupling with phonons are near the Fermi surface of each band, changes in energy eigenvalues $\Delta E^{i}(q)$ should be estimated at the corresponding Fermi points k^{i}_F. We determined these values by the interpolation of two results at symmetry points Γ and X, when the skeleton bond angles hypothetically extend from a tetrahedral angle to 120°. The dilatation ratio along the skeleton axis (Δ_l) is 0.06 by this skeleton deformation. The resulting deformation potentials for $(SiH)_x$ and $(SiMe)_x$ are given in Table II.

TABLE II. Calculated intraband and interband deformation potentials for $(SiH)_x$ and $(SiMe)_x$.

	Intra-σ-band $\Xi^{\sigma\sigma}_{\rm eff}$ (eV)	Intra-π-band $\Xi^{\pi\pi}_{\rm eff}$ (eV)	Inter-σ-π-band $\Xi^{\sigma\pi}_{\rm eff}$ (eV)
SiH	6.2	0.67	5.5
SiMe	4.8	0.83	4.0

IV. PEIERLS INSTABILITY IN POLYALKYLSILENE

A. Phonon softening

As mentioned in Sec. III D, lattice-skeleton atom displacements towards the skeleton axis generate important phonon modes for electron-phonon coupling, although phonon modes relating to side groups do not. Analogous longitudinal-phonon modes are also generated in a linear lattice chain, which is formed by hypothetically extending skeleton bond angles of transplanar polymers to 180°. Therefore, we describe the phonon dispersion w_q without side groups in terms of the linear lattice model (Si skeleton). We also include two skeleton atoms in the unit cell of such a linear lattice model, because the transplanar zigzag chain (D_{2h} or C_{2h}) has two skeleton atoms in its unit cell. Phonon frequency w_q for this Si skeleton is then given by

$$w_q=\frac{2f}{M}\{1\pm[1-\sin^2(qa/2)]^{1/2}\}$$
$$=(w^{\rm sk}_0)^2\{1\pm[1-\sin^2(qa/z)]^{1/2}\}\ . \tag{4.1}$$

The next problem is to estimate the value of $w^{\rm sk}_0$. A transplanar zigzag chain can be found in the (110) plane of the diamond-type Si crystal. Each Si-skeleton chain in the crystallized Si has Si side groups, which are themselves to become skeletons of other Si chains. Thus, each skeleton chain connects to a Si tetrahedral network via bindings of Si side groups. However, for phonon modes towards the [110] direction, each Si skeleton vibrates in phase with respect to other Si skeletons. This means that Si-network side groups do not affect the Si skeleton and that the phonon frequency of the transplanar zigzag Si skeleton can be estimated from that of crystallized Si towards the [110] direction. Using this information, $w^{\rm sk}_0$ of Eq. (4.1) can be given as follows,

$$w^{\rm sk}_0=\sqrt{2}w^{\rm sk}_0=w^{[110]}_{q=0}=\left[\frac{8\alpha}{M_{\rm Si}}\right]^{1/2}, \tag{4.2}$$

with

$$\alpha=ac_{11}\ .$$

Here, a is the lattice constant of Si diamond-type crystal and c_{11} is the elastic constant.

When H atoms connect to the Si skeleton, H side groups seem to move in phase with respect to the skeleton Si because of the lightness of the H mass and tight binding to the skeleton. In this case, the effective skeleton mass can be used to take account of the influence of H side groups. The phonon frequency is then reduced as

$$w_0^{\mathrm{SiH}} = \left[\frac{M_{\mathrm{Si}}}{M_{\mathrm{Si}} + M_{\mathrm{H}}} \right]^{1/2} w_0^{\mathrm{sk}} . \tag{4.3}$$

Since C side groups tightly bind to the Si skeleton [$E^{\mathrm{Si\text{-}H}} = 294.6$ kJ/mol and $E^{\mathrm{Si\text{-}C}} = 290$ kJ/mol (Ref. 11)], a similar treatment would be applied for $(\mathrm{SiMe})_x$,

$$w_0^{\mathrm{SiMe}} = \left[\frac{M_{\mathrm{Si}}}{M_{\mathrm{Si}} + M_{\mathrm{C}}} \right]^{1/2} w_0^{\mathrm{sk}} . \tag{4.4}$$

The band overlapping causes a characteristic phonon softening that would not appear in the single-band structure. Figure 5 shows an example of phonon softening, provided that $m_\pi^* = 0.8$ and $m_\sigma^* = 1$ and that the ratio between the intraband and interband electron-phonon coupling constants ($g_{\mathrm{inter}}/g_{\mathrm{intra}}$) is 0.5. Three types of scattering processes cause three Kohn anomalies at the corresponding wave vectors of $q_\sigma = 2k_F^\sigma$, $q_\pi = 2k_F^\pi$, and $q_{\sigma\pi} = k_F^\sigma + k_F^\pi = \pi/a$, respectively. In the above condition, a single giant Kohn anomaly with $\Omega_q = 0$ is seemingly produced by intra-σ-band scattering. However, this single giant Kohn anomaly at q_σ causes not only a charge-density wave (CDW) having an incommensurate wave number of q_σ (σ CDW), but also that having an incommensurate wave number of q_π (π CDW). The reason is that there is an intrinsic relation between the incommensurate σ CDW and the incommensurate π CDW in the one-dimensional overlapping bands.

Coupled phonons due to the intra-σ-band scattering ($q_\sigma = 2k_F^\sigma$) relate to those due to the intra-π-band scattering ($q_\pi = 2k_F^\pi$) as

$$q_\sigma = 2\pi/a - q_\pi = K - q_\pi = q_\pi \tag{4.5}$$

because the one dimensionality of the overlapping bands results in the relation of $k_F^\sigma = \pi/a - k_F^\pi$. Therefore, coupled phonons having q_σ are equivalent to those having q_π and vice versa. This means that in a one-dimensional system with a band-overlap structure, two characteristic intraband Peierls instabilities are not independently but simultaneously generated, even when one of the two types of phonon modes (q_σ or q_π) starts to be singly softened. After the simultaneous opening of two Peierls gaps, the resulting system changes to an insulator.

The one dimensionality of the overlapping bands also results in that the interband-σ-π scattering generates a commensurate CDW ($\sigma\pi$ CDW). This commensurate CDW ($q_{\sigma\pi} = k_F^\sigma + k_F^\pi$) is produced by a dimerization of two skeleton unit cells and opens two Peierls gaps in both σ and π bands. The resulting system also becomes an insulator.

B. Metal-insulator Peierls transition

Figure 6 shows a M-I phase diagram of $(\mathrm{SiH})_x$ at room temperature. The values for intraband overlap functions G^{ii} are assumed to be equal ($G^{\sigma\sigma} = G^{\pi\pi}$). Band overlapping in the one-dimensional system causes two intraband scattering processes (intra-σ-band and intra-π-band scattering) and one interband scattering process (inter-σ-π-band scattering). These multiple-scattering processes produce three corresponding M-I transition lines. Thus, five "subphases" are seemingly able to appear in a polysilene phase diagram at room temperature (see Table III).

The following is a detailed discussion of five apparent subphases. In subphase I the smallness of the overlap functions for both intraband and interband scatterings effectively reduces the corresponding electron-phonon coupling constants. Although Kohn anomalies due to intra-σ- and π-band and inter-σ-π-band scattering are found, no static lattice displacements appear. Consequently, the system still remains metallic in this subphase I. In subphase II the electron-phonon coupling between σ electrons and q_σ phonons is strengthened and an in-

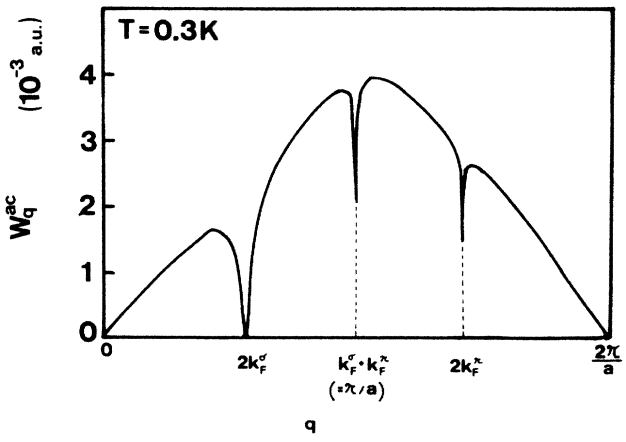

FIG. 5. Calculated phonon softening of $(\mathrm{SiH})_x$, $T = 0.3$ K, by extended Brillouin-zone representation. a.u. are atomic units with $\hbar^2 = 1$, $m_0 = \frac{1}{2}$, and $e^2 = 2$.

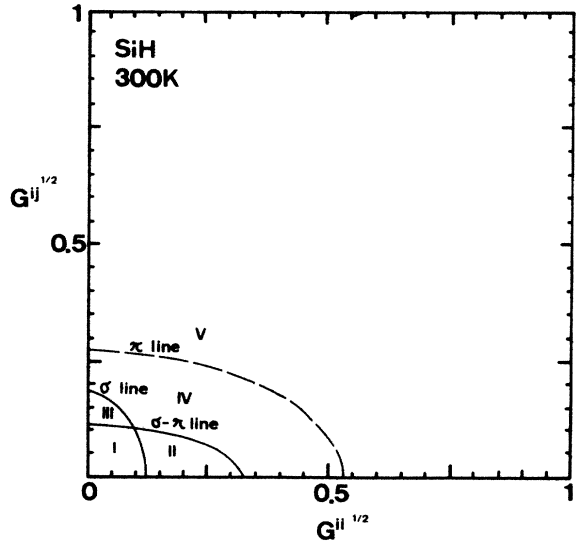

FIG. 6. Phase diagram for $(\mathrm{SiH})_x$ as function of intraband (G^{ii}) and interband (G^{ij}) overlap functions. Solid lines are resulting M-I transition lines. Subphase characterization is given in Table III.

TABLE III. Character of resulting five subphases expected in polysilene at 300 K. Symbols "inc," "com," "M," and "I" indicate "incommensurate," "commensurate," "metal," and "insulator," respectively.

	CDW Wave number	com. or inc.	Peierls gap	Metallic electrons	M or I
I				σ π	M
II	$q_\sigma = K - q_\pi$	inc	$P_\sigma > P_\pi$		I
III	$q_{\sigma\pi}$	com	P_σ, P_π		I
IV	$q_\sigma = K - q_\pi$ $q_{\sigma\pi}$	inc com	P_σ, P_π		I
V	q_σ or q_π $q_{\sigma\pi}$	inc inc com	P_σ P_π		I

commensurate CDW (σ CDW, equivalent to π CDW) appears. This σ CDW opens Peierls gaps not only in the σ band but also in the π band (Sec. IV A). As the width of the Peierls gap depends on the degree of electron-phonon coupling, a Peierls gap in the σ band (P_σ) wider than that in the π band (P_π) can be found in subphase II. The resulting insulator gap is attributed to the narrow P_π gap (Fig. 7). In subphase III the inter-σ-π-band scattering produces a commensurate CDW ($\sigma\pi$ CDW) with $q_{\sigma\pi} = k_F^\sigma + k_F^\pi = \pi/a$ but does not produce an incommensurate CDW. This commensurate CDW simultaneously opens Peierls gaps both in σ and π bands, and the system also becomes an insulator.[12] The resulting band structure is shown in Fig. 8. Subphase IV and V are insulators, which have also Peierls gaps in the σ and π bands. The incommensurate CDW (σ CDW equal to π CDW) and the commensurate CDW ($\sigma\pi$ CDW) compete in these subphases (IV and V). Since polyalkylsilene has a much larger intra-σ-band coupling constant ($\Xi_{\text{eff}}^{\sigma\sigma}$) than its intra-$\pi$-band coupling constant ($\Xi_{\text{eff}}^{\pi\pi}$) (Sec. III D), the resulting intraband M-I transition line is characterized by that due to intra-σ-band scattering (σ line). The final M-I transition line due to intraband scattering is then reduced to the σ line in polyalkylsilene. Thus, at room temperature, polysilene might have the capability of four subphases, divided by the intraband M-I line (σ line) and the interband M-I line ($\sigma\pi$ line).

For the ideal polysilene having a highly symmetry (D_{2h} or C_{2h}), the normality and orthogonality between the σ and π bands guarantee $G^{ii}=1$ and $G^{ij}=0$. Here, we assume that G^{ij} is zero, a value precluding interband scattering, and investigate the influence of intraband

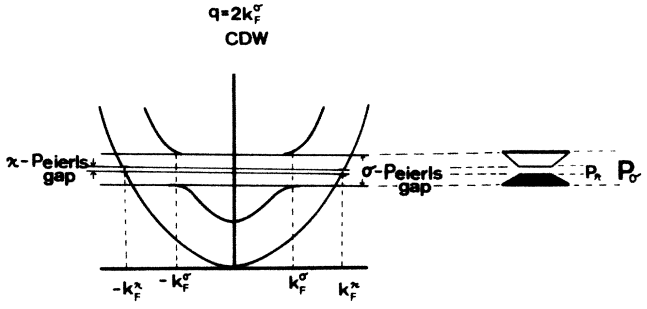

FIG. 7. Illustration of resulting Peierls-gap structure caused by σ CDW.

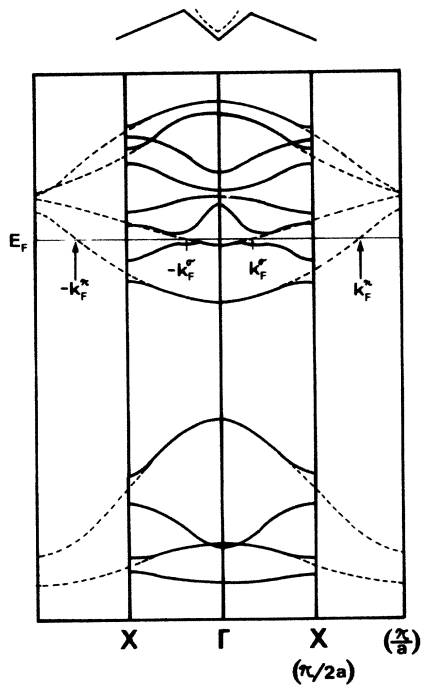

FIG. 8. Illustration of resulting band structure caused by dimerization of two unit cells [i.e., generating commensurate Peierls instability ($\sigma\pi$ CDW)].

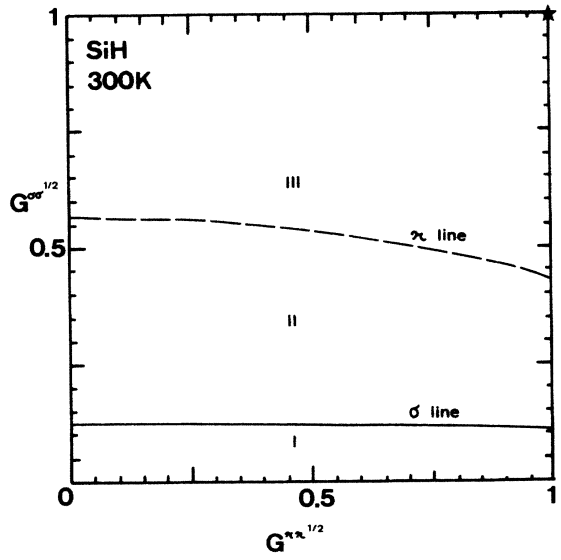

FIG. 9. Phase diagram of $(SiH)_x$ at 300 K, as function of intra-σ-band (G^{σ}) and intra-π-band ($G^{\pi\pi}$) overlap functions. Solid lines also correspond to M-I transition lines. ★ located at top right-hand corner means the position for ideal polysilyne having D_{2h} symmetry with $G^{ii}=1$ and $G^{ij}=0$.

scattering on the M-I transition by varying values for intraband overlap function G^{ii} ($G^{\sigma\sigma}$ and $G^{\pi\pi}$) as parameters.

Figure 9 shows the M-I phase diagram of $(SiH)_x$ at room temperature. $(SiH)_x$ has the following three subphases. Metallic electrons in σ and π bands make subphase I a metal. In subphase II the incommensurate σ CDW, equivalent to π CDW, is generated. Therefore, two Peierls gaps open in the π band as well as in the σ band. Subphase III is also an insulator phase with the

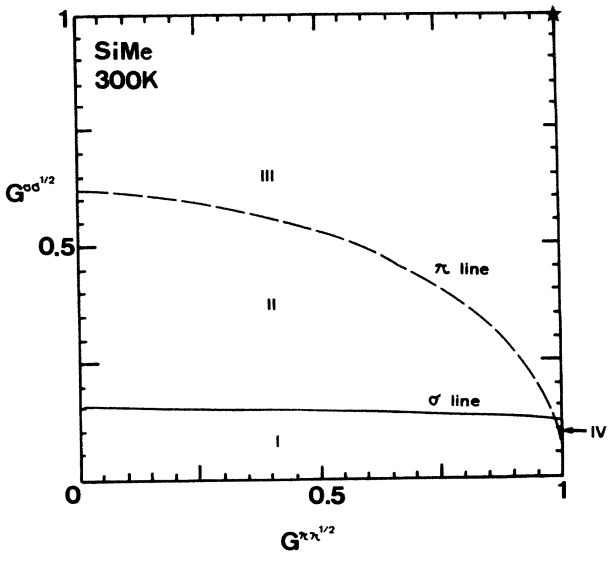

FIG. 10. Corresponding phase diagram of $(SiMe)_x$, as function of intra-σ-band ($G^{\sigma\sigma}$) and intra-π-band ($G^{\pi\pi}$) overlap functions.

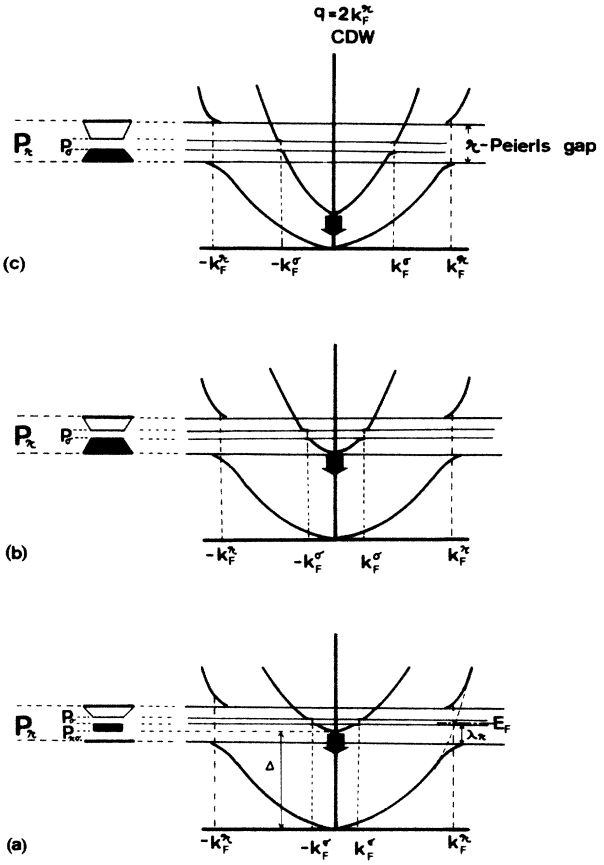

FIG. 11. Illustration of Peierls gap structure caused by π CDW, as a function of degree of band overlapping.

presence of the incommensurate $\pi(\sigma)$ CDW.

In real polymers, the reduction in symmetry due to thermal skeleton winding decreases the value of the intraband overlap function G^{ii} from unity and increases that of the interband one, G^{ij}, from zero. Although these random windings render the position of the real polymer ambiguous in the phase diagram, the corresponding position would seem to close to the resulting M-I transition zone, approaching along a line with a unit slope ($G^{\sigma\sigma}/G^{\pi\pi}=1$) from the ideal position (see ★ in Fig. 9). The reason is that amount of reduction in G^{ii} would seem to be equal in the σ and π bands. Therefore thermal skeleton winding might play a role of the suppression for Peierls M-I transition.

We now consider the influence of side-group methylation. The M-I phase diagram for $(SiMe)_x$ is given in Fig. 10. $(SiMe)_x$ has four subphases. Three of these subphases, I–III, are similar to those in $(SiH)_x$. Since the intra-π-band deformation potential of $(SiMe)_x$ is greater than that of $(SiH)_x$, a novel subphase IV appears. In this subphase an incommensurate $\pi(\sigma)$ CDW is generated and Peierls gaps are opened in the σ band as well as in the π band so as to transit the system to an insulator. However, the details of the Peierls-gap structure are different from those subphase II and depend upon the degree of band overlap (see the Appendix). This subphase

IV tends to extend with lowering temperature because of the narrowed subphase II.

The side-group methylation produces the following two features. One is a change in the deformation-potential values. The side-group substitution from an H atom to a Me group reduces all of the deformation potentials (Ξ^{ij}_{eff}, $i,j=\sigma,\pi$) except for $\Xi^{\pi\pi}_{\text{eff}}$. These reduced deformation potentials weaken the corresponding electron-phonon couplings. This causes the comparative extension of the metallic phase. The other influence is an additional one, which appears in the overlap functions via thermal rotation of side groups. The random rotation of Me groups easily reduces the symmetric character of the polymer and then nonorthogonal AO's are nonsymmetrically admixtured. Similar to the thermal skeleton winding, this thermal side-group rotation decreases the value of G^{ii} from unity and increases that of G^{ij} from zero. However, this nonsymmetrical admixture, of nonorthogonal AO's cannot occur for H-atom side groups because $1s$ AO's of H atoms have a spherical symmetry about side-group rotation. Therefore, methylation might enhance the metallic character of $(SiMe)_x$ over that of $(SiH)_x$.

ACKNOWLEDGMENTS

We would like to express our thanks to Dr. T. Ohno, Dr. Y. Tokura, Dr. N. Matsumoto, Dr. A. Sugimura, and Dr. K. Sugii for their fruitful discussions.

APPENDIX

Let λ_π be the energy lowering of the π band due to the Peierls-gap opening. In the case of

$$\frac{\hbar^2}{2m_\pi}(k_F^\pi)^2-\lambda_\pi\le\Delta\ , \tag{A1}$$

intruding σ states are formed in the resulting wide Peierls gap of the π band (P_π) [Fig. 11(a)]. Therefore, the resulting insulator has a gap $P_{\pi\sigma}$ in addition to the normal Peierls gaps of P_π and P_σ. The increases in the band overlap (i.e., reduction in Δ) decrease the width of the gap $P_{\pi\sigma}$ and the occupied σ states tend to delocalize.

If the following relation is satisfied by increasing the band overlap,

$$\frac{\hbar^2}{2m_\pi}(k_F^\pi)^2-\lambda_\pi=\Delta\ , \tag{A2}$$

the wider gap of P_π is just covered by a σ-band state with a narrow gap of P_σ [Fig. 11(b)]. The resulting insulator seems to have a narrow gap of P_σ. However, the electronic character of the occupied states semimetallically changes from the π-like one to the σ-like one at $E=\Delta$.

When these two bands overlap strongly, and they exceed the following condition,

$$\frac{\hbar^2}{2m_\pi}(k_F^\pi)^2-\lambda_\pi>\Delta\ , \tag{A3}$$

an insulator having a narrow gap of P_σ results. In the valence states below Δ, σ electrons and π electrons degenerate in this case [Fig. 11(c)].

---

[1]Following the carbon analog, we denote here polymers of $+SiH_2—SiH_2+_x$, $+SiH=SiH+_x$, and $+Si\equiv Si+_x$ as polysilane, polysilene, and polysilyne, respectively.

[2]K. C. Pandey, Phys. Rev. Lett. **28**, 1913 (1981).

[3]M. J. Fink, M. J. Michalczyk, K. J. Heller, R. West, and J. Michel, J. Chem. Soc. Chem. Commun. 1010 (1983).

[4]K. Takeda (unpublished).

[5]K. Takeda, H. Teramae, and N. Matsumoto, J. Am. Chem. Soc. **108**, 8186 (1986).

[6]J. C. Slater and G. F. Koster, Phys. Rev. **94**, 1498 (1954).

[7]W. A. Harrison, *Electronic Structure and the Properties of Solids* (Freeman, San Francisco, 1979).

[8]At $T=0$ K, the electron number density (n) is defined in terms of the DOS (g^t) and the Fermi-Dirac distribution function ($f^{T=0}_{(E)}$) as $n=\int_0^{E_F} g^t_{(E)} f^{T=0}_{(E)} dE$. By inserting Eq. (2.6) into the above equation, the following equation can be obtained:

$$\left[\frac{2m_\pi}{\hbar^2}\right]^{1/2}(E_F)^{1/2}+\left[\frac{2m_\sigma}{\hbar^2}\right]^{1/2}(E_F-\Delta)^{1/2}=\frac{\pi n}{2}\equiv k_{F_0}\ .$$

[9]The value of m_π is restricted owing to the overlapping of the π and σ bands as follows: $m_\pi\le\hbar^2k_{F_0}^2/2\Delta$. The value of m_σ is also restricted by the real value condition of Fermi energy, $m_\sigma\ge m_\pi-\hbar^2k_{F_0}^2/2\Delta$.

[10]D. Pine and D. Nozières, *The Theory of Quantum Liquids* (Benjamin, New York, 1966), p. 235; H. Kamimura, Ōyōbutsuri **45**, 616 (1976).

[11]*Chemical Handbook* (Maruzen, Tokyo, 1975) (in Japanese).

[12]A. J. Berlinsky, J. Phys. C **9**, L283 (1976).